Trends in Cell Biology

CellPress

Feature Review

Mechanobiological approaches to synthetic morphogenesis: learning by building

Marija Matejčić[1,*] and Xavier Trepat[1,2,3,4,*]

Tissue morphogenesis occurs in a complex physicochemical microenvironment with limited experimental accessibility. This often prevents a clear identification of the processes that govern the formation of a given functional shape. By applying state-of-the-art methods to minimal tissue systems, synthetic morphogenesis aims to engineer the discrete events that are necessary and sufficient to build specific tissue shapes. Here, we review recent advances in synthetic morphogenesis, highlighting how a combination of microfabrication and mechanobiology is fostering our understanding of how tissues are built.

Synthetic morphogenesis at the interface of engineered and self-organized tissues

The field of synthetic morphogenesis encompasses research focusing on artificially building living structures of defined shapes. Rather than observing how living systems *in vivo* or in isolation self-assemble [1], synthetic morphogenesis guides these processes by tightly controlling properties, such as differentiation [2], positioning components [3], or mechanics [4,5]. Hence, it aims to identify the structural demands of developing tissues to ensure their stability and function, and examines their limits by, for example, changing size or shape [6–8]. In addition, the tools and model systems it uses may allow synthetic morphogenesis to build shapes that do not occur naturally or occur in diseased states [7]. Through this approach, alternative developmental paths can be investigated to be applied to regenerative medicine or engineering fields, such as soft robotics.

The term 'morphogenesis' can be applied to many levels at which shape generation occurs, from protein folding to whole-body formation. In this review, we focus on the tissue scale, which examines the cell-driven morphogenesis of animal tissues. We exclude the fields of bioprinting (reviewed in [9]) and organ-on-chip systems (reviewed in [10–13]), which generally aim at complexity and application. Instead, we highlight elementary systems and processes, with an emphasis on how mechanics enables shape control and tissue function in epithelia. Given that the field of tissue mechanics has boomed over the past decade or so [14,15], we suggest that it is important to catalog advances in, and identify major current and future challenges for, combining tissue mechanics with synthetic morphogenesis, helping to focus community efforts.

Building elementary living shapes

Early studies attempted to artificially build living shapes by growing tissues on synthetic substrates that mimic natural morphology or by releasing naturally occurring geometric constraints. Examples include the growth of bone tissue on a synthetic sponge [16] or the removal of the enveloping egg follicle to obtain spherical insect eggs from naturally elongated ones and study the effect of shape change on development [17]. Building on such early research, current synthetic tissue morphogenesis lies at the intersection of developmental cell biology, bioengineering, materials science and physics (Box 1) and uses methods that include biophysics tools, genetic modification, microscopy, detailed quantitative analyses, and simulations.

Highlights

Advances in the field of epithelial tissue mechanics enable synthetic morphogenesis to build tissue systems the mechanical properties of which can be controlled and measured.

Canonical epithelial models, such as Madin–Darby canine kidney epithelial cells (MDCK) cells, are being used to develop new devices to stretch and compress tissues or change tissue curvature.

More recent tissue systems, such as those based on induced pluripotent stem cells (iPSCs) and organoids, are used in minimal set-ups to study tissue self-organization, including cell positioning and cell fate.

Growing the same tissue in minimal 2D and 3D environments showed that the third spatial dimension is not required for some aspects of tissue self-organization.

Synthetic substrates and protein patterning allow tissues to be grown with a defined size and shape. Using stem cells, these have applied to demonstrate in a highly controlled way how initial tissue geometry and tissue mechanics affect the morphogenetic outcome.

[1]Institute for Bioengineering of Catalonia (IBEC), The Barcelona Institute for Science and Technology (BIST), Barcelona, Spain
[2]Facultat de Medicina, Universitat de Barcelona, Barcelona, Spain
[3]Institució Catalana de Recerca i Estudis Avançats (ICREA), Barcelona, Spain
[4]Centro de Investigación Biomédica en Red en Bioingeniería, Biomateriales y Nanomedicina (CIBER-BBN), Barcelona, Spain

*Correspondence:
mmatejcic@ibecbarcelona.eu (M. Matejčić) and
xtrepat@ibecbarcelona.eu (X. Trepat).

© 2022 Elsevier Ltd. All rights reserved.

Box 1. Epithelial mechanics

The rational engineering of epithelial shapes requires an understanding (and eventually a measurement) of the state of mechanical stress at every point of the epithelial surface. As a first approximation, an epithelium can be considered as a flat or curved membrane that supports a 2D state of stress tangential to its surface. This approximation is valid when the epithelial thickness is smaller than other relevant dimensions of the system (such as the lumen diameter) and when apicobasal tension asymmetries, bending moments, or tissue spontaneous curvature can be neglected. The state of stress of the epithelium is then provided by a 2×2 matrix, called the stress tensor. Given that this stress tensor is symmetric, two privileged, mutually orthogonal, directions exist at every point of the epithelium, along which stress is maximal and minimal, respectively.

For elementary geometries such as those discussed in section 'Building elementary living shapes' in the main text, the stress tensor adopts a simplified form. In the case of a sphere or a spherical dome of radius R, stress is uniform and isotropic, that is, it has the same value in every position and in every direction of the epithelium. The stress tensor then simplifies to a single scalar value, the epithelial surface tension σ, which is balanced by pressure in the lumen ΔP (Figure IA) and can be readily computed using Laplace's law (Equation I):

$$\sigma = \frac{\Delta P}{2} R \qquad [I]$$

If epithelial shape deviates from a sphere but is symmetric about one axis, then the two principal stress directions are the circumferential and meridional directions (Figure IB). Tension along these directions can be computed using Equations II and III [142]:

$$\sigma_c = \frac{\Delta P}{2}\left(2 - \frac{R_c}{R_m}\right) \qquad [II]$$

$$\sigma_m = \frac{\Delta P}{2} R_c \qquad [III],$$

where σ_c and σ_m are stress values in the circumferential and meridional directions, respectively, and R_c and R_m are the local radii of curvature along those directions, respectively.

Besides luminal pressure and shape, the stress in the epithelium is also determined by the traction forces applied at the cell–substrate interface. In the case of a flat monolayer, mechanical equilibrium can be invoked to infer epithelial stress from the direct measurement of traction forces in a technology called 'monolayer stress microscopy' [143]. However, for a curved monolayer, no method has yet been developed to generalize this approach.

In some morphogenetic processes, the membrane approximation discussed above is not applicable. For example, this is the case of budding of the vertebrate intestinal crypt or ventral furrow formation during *Drosophila* gastrulation. In these processes, stresses normal to the epithelial surface are generated to drive out-of-plane deformations. One mechanism to generate out-of-plane stresses is an asymmetry between apical and basal contractility, which results in epithelial bending. Alternatively, out-of-plane stress can arise from buckling instabilities (see section 'Engineering tissue folding' in the main text).

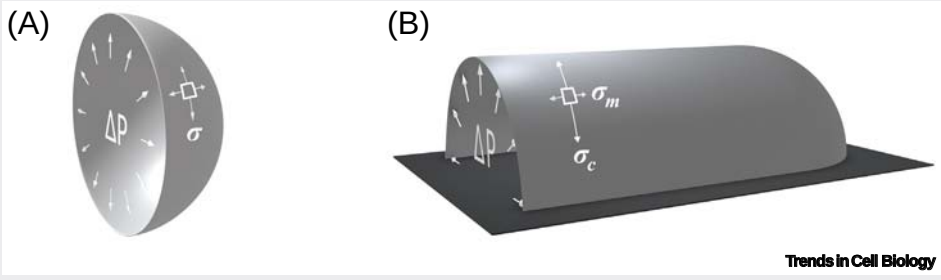


Figure I. Stress diagrams in curved epithelial sheets modeled as thin membranes. (A) Pressure and stress tensor in a spherical epithelial sheet with a fully closed lumen. Stress is uniform and isotropic along the surface (surface tension σ) and balanced by pressure in the lumen ΔP. (B) Pressure and stress tensor in an axisymmetric, nonspherical curved epithelium. Stress is distributed along two principal directions, the circumferential (tension σ_c) and meridional (tension σ_m).

Glossary

Embryonic stem cells (ESCs): pluripotent cells isolated from preimplantation embryos. They have the potential to differentiate into all three embryonic germ layers and their derivatives.

Epithelial–mesenchymal transition (EMT): a process of epithelial cells losing epithelial characteristics, such as cell polarity and adhesion to neighbor cells. Cells acquire a migratory and/or invasive behavior. EMT is a hallmark of developmental and homeostatic processes, as well as of cancer metastasis initiation.

Extracellular matrix (ECM): network of proteins, such as collagen, laminin, or fibronectin, building the protein stromal meshwork to which cells attach and through which they migrate. ECM composition, organization, and stiffness affects cells, such as their behavior and fate. Commercial sources include Matrigel and Basement Membrane Extract (BME).

Gelatin methacryloyl (GelMA): modified gelatin (hydrolyzed and denatured collagen) hydrogel produced through the reaction of gelatin with methacrylic anhydride (MA), photocrosslinked (UV). As a tissue substrate, it can be degraded and bound by cells, because the MMP and RGD sequences are preserved.

Human umbilical vein endothelial cells (HUVECs): human cell line widely used to study the formation and development and pathology of blood or lymphatic vessels. HUVECs originate from the umbilical cord endothelium.

Induced pluripotent stem cells (iPSCs): type of PSC generated from differentiated somatic cells. Somatic cells can be converted into PSCs using the four Yamanaka factors (transcription factors Myc, Oct3/4, Sox2, and Klf4).

Madin–Darby canine kidney epithelial cells (MDCK): mammalian cell line, widely used in biomedical and biophysical research. MDCK originate from a kidney tubule of a dog.

Matrix metalloprotease (MMP): calcium-dependent protease degrading ECM proteins. It is also able to degrade other molecules, such as specific cell surface receptors.

Norland Optical Adhesive (NOA): clear, colorless, liquid photopolymer that cures when exposed to UV light.

Polyacrylamide (PAA): hydrogel used in tissue mechanics research to fabricate

Epithelial monolayers are the starting point of most synthetic morphogenesis studies (Figure 1). Their junctions and defined polarity allow them to be patterned [4,18,19], stretched [20,21], or compressed [22,23] to uncover basic mechanical features of tissue architecture and function, which are all

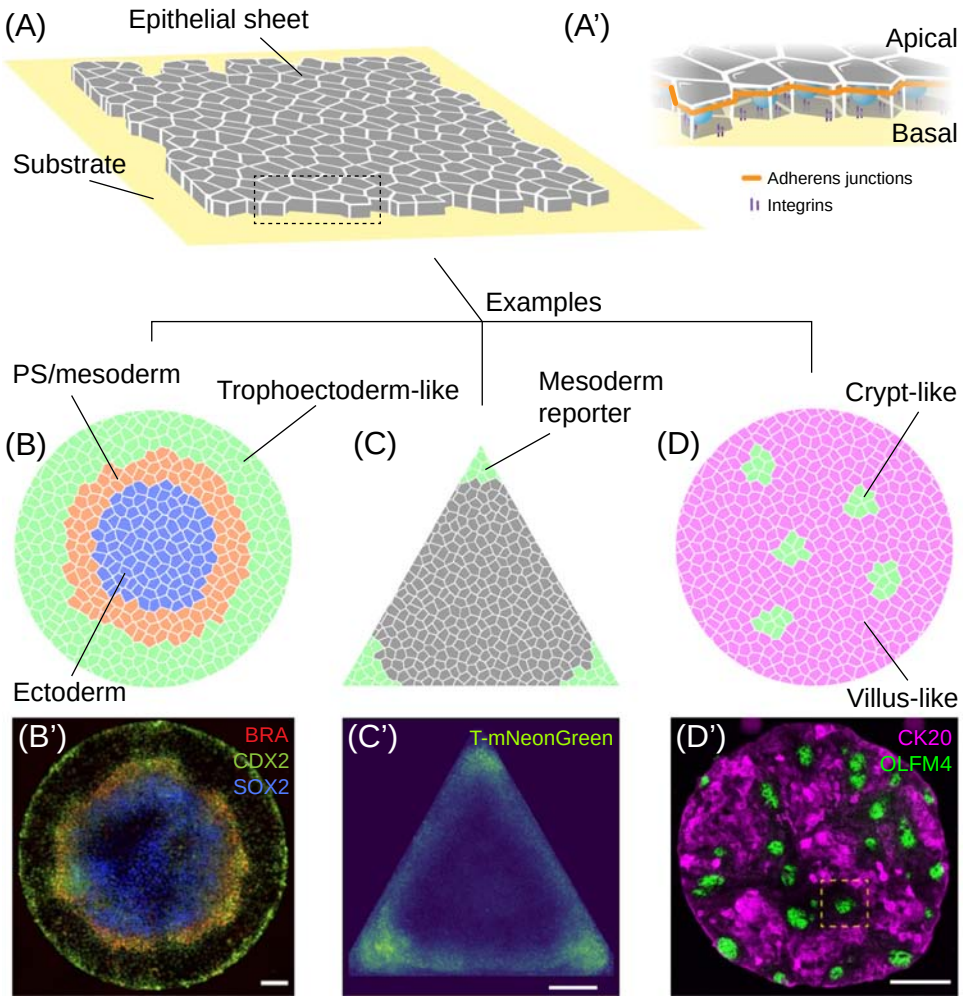


Figure 1. Examples of flat epithelial monolayers to study the mechanics of morphogenesis. (A) Epithelial monolayers grown on flat natural or synthetic substrates can be patterned into desired shape and size. This is achieved by patterning molecules that promote cell–substrate adhesion, such as specific extracellular matrix (ECM) proteins, by different methods (see Box 2 in the main text). An epithelium growing on a rectangular pattern is shown. (A') A small region of an epithelial monolayer [dashed line in (A)], showing basic epithelial junctional organization that impacts epithelial shapes and the polarity of built structures. Cells are bound to each other by apical (adherens) junctions and lateral junctions (only apical shown), and attach to the substrate at their basal side through integrins. (B) Schematic of a flat model of gastrulation, the gastruloid, with germ layer-like regions labeled. The correct organization of this tissue depends on the monolayer size. (B') Fluorescence microscopy image of a human embryonic stem cell (hESC) immunostaining corresponding to the scheme in (B). Scale bar: 100 μm. (C) Schematic of a monolayer of hESCs grown on triangular patterns. High tension develops in triangle tips, triggering the expression of a live mesoderm reporter T(brachyury). (C') Fluorescence microscopy image of an hESC triangular monolayer 30 h after BMP4 addition, corresponding to the scheme in (C). Signal has been normalized 0–1. Scale bar: 250 μm. (D) Schematic of a monolayer of mouse small intestinal organoids grown on circular patterns. Despite its 3D geometry *in vivo*, the intestinal epithelium compartmentalizes *de novo* into crypts and villi-like regions on flat, 2D substrates. (D') Fluorescence microscopy image of immunostained mouse intestinal organoid, with stem cells labeled in olfactomedin 4 (green) and differentiated cells with cytokeratin 20 (magenta). Corresponding to the scheme in (D). Scale bar: 200 μm. Adapted, with permission, from [6] (B') and [4] (C'); adapted from [39] (D'). Abbreviation: PS, primitive streak.

custom cell substrates of varying stiffness (0.3–300 kPa). Fluorescent microspheres can be incorporated in its bulk to track gel displacements and calculate cell–substrate traction forces.

Polydimethylsiloxane (PDMS): silicone-based organic polymer used in tissue mechanics research to fabricate custom cell substrates, including microfluidic channels. Fluorescent microspheres can be attached onto its surface to track gel displacements and calculate cell–substrate traction forces.

Polyethylene glycol (PEG): hydrogel used in tissue mechanics research to fabricate custom cell substrates; can be prepared to contain cell-binding motifs (RGD) in bulk or to be hydrolytically degraded by the MMPs of the cells. Stiffness varies, being 0.5–5 kPa for cell-degradable or 20–500 kPa for nondegradable crosslinkers.

Polyethylene glycol diacrylate-acrylic acid (PEGDA-AA): hydrogel made from poly(ethylene glycol) diacrylate (PEGDA) and acrylic acid (AA); used to fabricate substrates with custom topology and mesh size that allow diffusion and gradient formation with biochemical factors of choice.

important in the control of synthetic shapes. Typical studies in synthetic morphogenesis use established epithelial cell lines, such as **Madin–Darby canine kidney epithelial (MDCK) cells** (see Glossary) e.g., [24]) and endothelial cells (e.g., [25]), or organ-specific cultures, such as colon epithelial cells [26]. More recently, studies began leveraging the power of animal stem cells, including **induced pluripotent stem cells** (iPSCs) [27], **embryonic stem cells** (ESCs) [6], or ESC-like populations [28], to study embryogenesis across the phylogenetic tree (reviewed in [28,29]). Differentiated organoids or live tissue explants [30] can also be seeded on specialized substrates or devices to guide their growth and shape. Here, we discuss the latest strategies using a variation of cell types and substrates to build the elementary geometric structures that form during the development of an organism, including flat sheets (Figure 1), spheres (Figure 2A,B), domes (Figure 2C), and tubes (Figure 2D,E).

Flat sheets

Although morphogenetic processes and the resulting shapes are typically thought about in three dimensions, studies demonstrated that many features integral to morphogenesis, such as tissue patterning, cell shape, or force distribution, are recapitulated in flat tissue configurations (Figure 1B–D) (reviewed in [31]). Flat tissue layers generated from human ESCs (Figure 1B,B′) recapitulated germ layer specification are termed '2D gastruloids' [6], akin to their 3D counterparts [32]. Circular **extracellular matrix** (ECM; Matrigel) patterns reduced the geometrical heterogeneity of these free-growing colonies and guided differentiation of human (h)ESCs into three germ layers and a trophoblast-like population. More specifically, tissue size controls the formation of gradients that direct germ layer differentiation, because BMP-4-based signaling gradient formed only in human blastocyst colonies that are large enough (i.e., radius 500 μm, but not 200 μm [33]). Growing the same cells on triangular patterns [4] localized high tension to the triangle tips (Figure 1C,C′). At these points, mesoderm tissue was specified through canonical Wnt signaling, demonstrating that both tissue size and tissue shape have a role in germ layer differentiation. Given their strictly defined geometry, such patterned tissues can also be used to asses geometry-independent sources of heterogeneity in development [34].

Aside from gastrulation mechanisms, micropatterning methods were used to study organ-specific development. Basics of human neurulation were recapitulated in 2D colonies of hESCs and hPSCs [35–37] and micropatterns were used as a base to grow a 3D tissue neurulation model (see 'Domes' section and [7]). Similarly to gastrulation, initial tissue shape and size were found to guide neural tube morphogenesis. Intestinal organoids also readily spread on flat substrates into enteroid monolayers or flat open-lumen organoids, and maintain the spatial organization and tissue patterning of the *in vivo* intestinal tissue. Growing such intestinal organoids on a thin Matrigel layer, an intrinsic WNT-BMP circuit was revealed to govern intestinal proliferation and organization [38]. On mechanically controllable substrates [**polyacrylamide** (PAA) hydrogels], flat organoids were patterned into large (700–900 μm) disks to standardize the monolayer size (Figure 1D,D′) [39]. Cell-substrate traction forces were mapped, as well as tension that compartmentalizes the intestinal tissue and drives cell migration out of the crypt. In addition, by modulating substrate stiffness, the authors showed that the flat organoid retained the ability to generate 3D intestinal crypts, because on soft substrates (<1.5 kPa), the crypt region indented through apical constriction of the stem cells. A softer substrate also resulted in more stem cells and a larger intestinal crypt [39,40].

Although 3D geometry can instruct cell differentiation and guide correct tissue organization based on curvature (Figure 3; see also the 'Engineering tissue folding' and 'Cell migration' sections), studies on morphogenesis in 2D show that not all morphogenetic processes require the third spatial dimension. For some investigations, such as those outlined above, questions can be answered by using more controllable, 2D-patterned tissues.

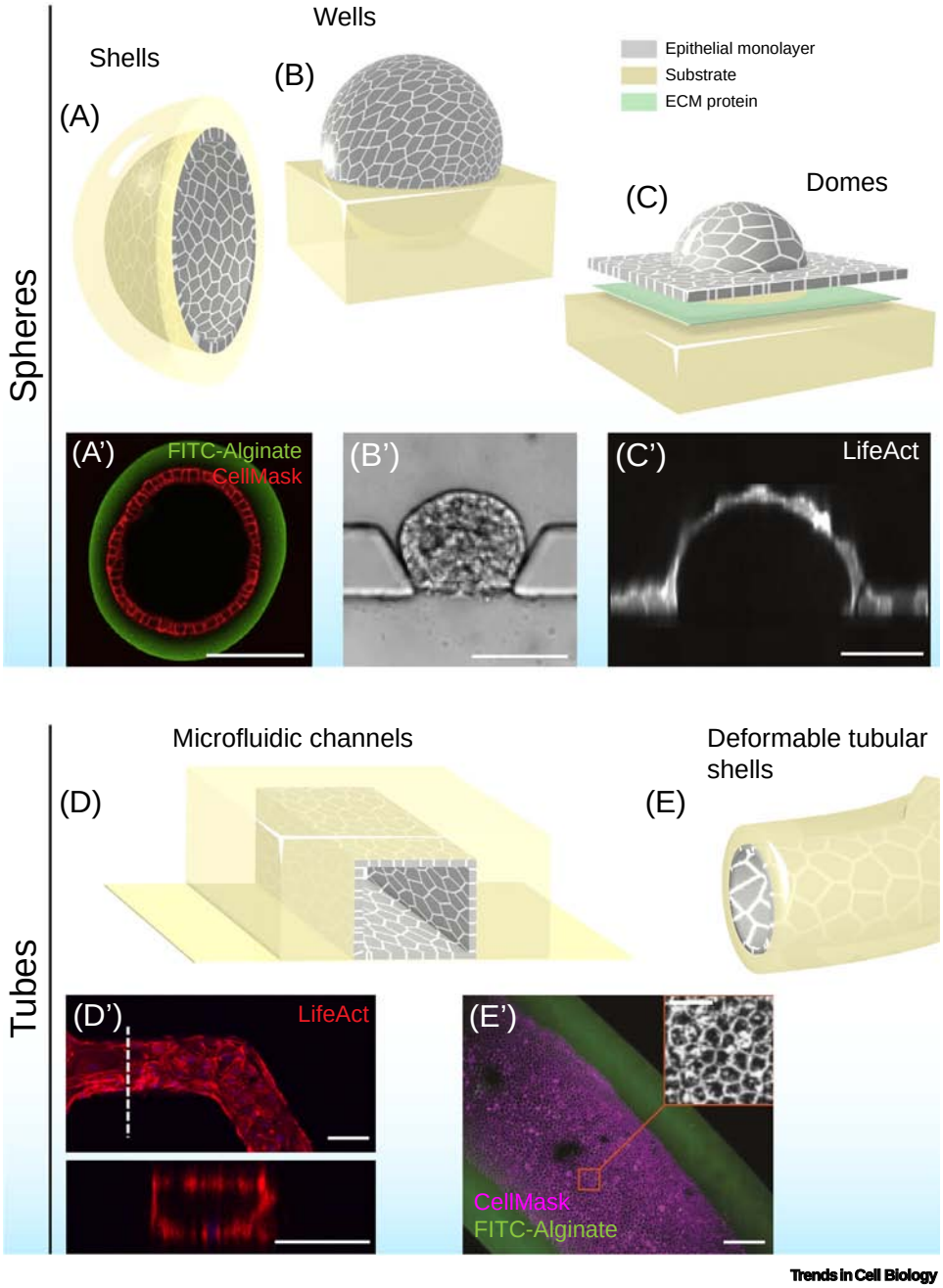


Figure 2. Substrate configurations for 3D synthetic morphogenesis. (A–C) Epithelial spheres. (A) Schematic of growing epithelial spheres in spherical confinements. The inner surface of these shells is typically coated with extracellular matrix (ECM) proteins, promoting basal attachment and resulting in an apical lumen in the center. (A') Fluorescence microscopy image of a monolayer of Madin–Darby canine kidney epithelial cells (MDCK) growing basally attached to a spherical alginate shell. Cell membranes are labeled in red and the alginate in green; corresponds to scheme in (A). Scale bar: 100 μm. (B) Schematic of growing epithelial spheres with the aid of microwells. These are typically low-adhesion wells, promoting cell aggregation. (B') Brightfield image of a human pluripotent stem cell (hPSC) cluster growing in an 80-μm Geltrex well embedded in a microfluidic device. These clusters undergo several landmark gastrulation-like events and can be used to study early stages of human post-implantation development; corresponds to scheme in (B). Scale bar: 80 μm. See main text for additional

(Figure legend continued at the bottom of the next page.)

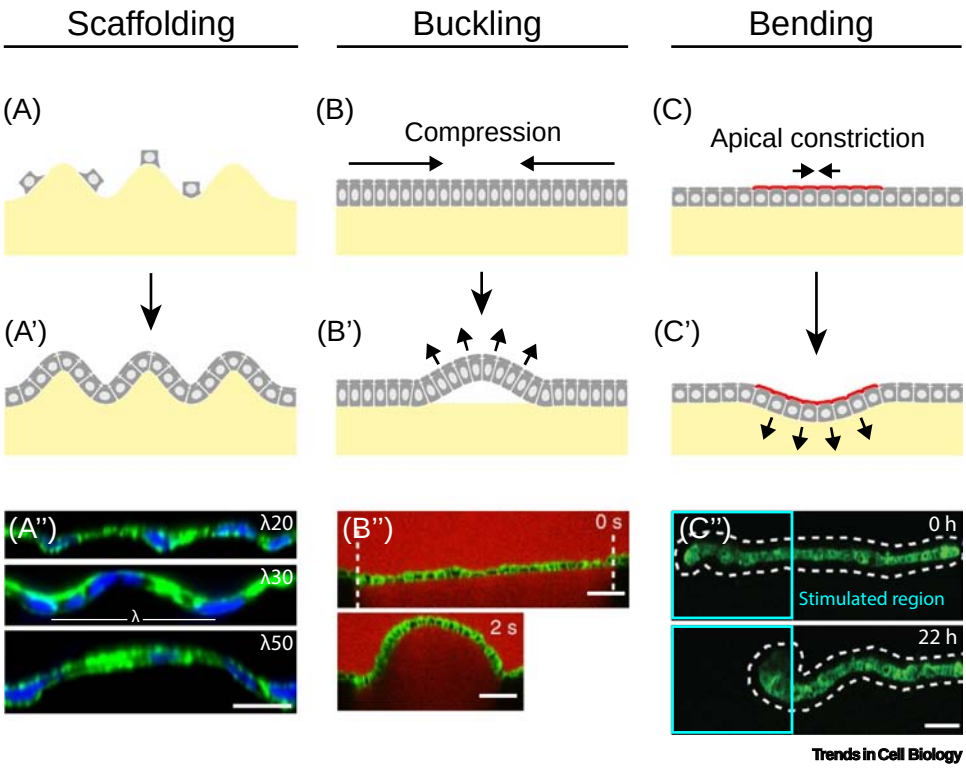


Figure 3. Generating epithelial folds. (A–A″) Using substrates with preformed folds. (A) Cells are seeded on top of the extracellular matrix (ECM)-coated substrate and, after reaching confluency (A′), assume the curvature determined by the substrate. (A″) Madin–Darby canine kidney epithelial cell (MDCK) monolayers grown on corrugated hydroxy-polyacrylamide with different wavelengths. Cells are thinner on top of substrate hills than in the bottom on valleys. Scale bar: 10 μm. (B–B″) Inducing epithelial buckling to generate folds. (B) The monolayer is laterally compressed by confined growth, prestretch or acute lateral compression, increasing pressure and cell density in the tissue. (B′) Past the point of buckling pressure, the buckling instability drives an out-of-plane deformation and fold generation. Detachment from the substrate (i.e., basal buckling) is illustrated. (B″) Buckling of a compressed suspended MDCK monolayer. Scale bars: 50 μm. (C–C″) Creating epithelial folds by localized cell constriction. Apical constriction is shown. (C) Apical actomyosin contractility is locally enhanced in a subset of cells in an epithelial monolayer (red). (C′) The actomyosin network of the stimulated cells constricts, decreasing the apical cell area and changing the cell shape. The resulting wedge-shaped cells deform the monolayer, indenting it into the substrate. (C″) Folding of an MDCK colony expressing GFP-NShroom3-iLID. Blue rectangle marks the blue-light stimulated region. Scale bar: 50 μm. Adapted, with permission, from [36] (A″) and [105] (C″); adapted from [118] (C″).

Spheres

Lumenized spheres are organ precursors during development (e.g., otic vesicles), functional structures in adult organs (e.g., eyes or bladder), and undesired shapes in disease (e.g., polycystic kidney disease). Epithelia can be guided into spherical shapes by artificially confining cells

examples. (C) Schematic of growing epithelial hemispheres as domes, with the aid of protein micropatterning (green) to create low-adhesion areas in the monolayer. (C′) Fluorescence microscopy image of a MDCK dome grown on a soft polydimethylsiloxane (PDMS) gel patterned with fibronectin; corresponds to scheme in (C). Scale bar: 50 μm. (D–E) Epithelial tubes. (D) Schematic of growing epithelial tubes using a microfluidic channel. These channels can be produced with a desired shape and size, typically from PDMS, mounted on glass. (D′) Fluorescence microscopy image of a **human umbilical vein endothelial cell** (HUVEC) tube grown in a microfluidic channel; corresponds to scheme in (D). Scale bars: 100 μm. (E) Schematic of growing epithelial tubes using a microfluidic channel. These channels can be produced with a desired shape and size, typically from PDMS, mounted on glass. (E′) Fluorescence microscopy image of an MDCK tube grown in a deformable alginate channel; corresponds to scheme in (E). Scale bar: 100 μm. Adapted, with permission, from [24] (A′), [56] (B′), and [59] (C′); adapted from [25] (D′) and [68] (E′).

(Figure 2A) or by enabling self-organization in mechanically defined substrates or on preformed molds (Figure 2B). In both cases, the lumen is typically apical, while the basal epithelial surface faces the environment. MDCK and human neural stem cells grown in spherical alginate shells [24,41] (Figure 2A,A′) enclose an apical lumen and were used to study growth-mediated compression and buckling pressure of epithelia (Figure 3B-B) (see 'Buckling' section and [24]). In unconfined 3D cultures, many cell types [42,43], including cancer cells [44], also self-assemble into spherical cysts. In intestinal organoids, a cystic shape is associated with a PSC state, devoid of differentiated cells, and differentiation implies budding out of the spherical structure. In this system, it was also discovered that intestinal stem cells proliferate better on substrates of intermediate (1.3 kPa) stiffness, than on softer (300 Pa) substrates [45]. Given that stiffness influences cell survival, fate, as well as tissue shape, it should be controlled in synthetic morphogenesis projects by using mechanically well-defined substrates.

Aside from specific organs, such as the intestine, embryogenesis of many animals is associated with a spherical shape. To study embryogenesis in synthetic systems, spherical structures reminiscent of early mammalian embryos, blastoids, were assembled *in vitro* (mouse [46–48], human [49–51]; reviewed in [52–54]) (Figure 2B,B′) and characterized as faithful models to study human implantation development [55,56]. In a microfluidic device, [56], blastoids from primed hESC clusters (Figure 2B′) developed until the onset of gastrulation (i.e., primitive streak formation). With protocols to assemble embryonic structures and control their luminal pressure [57,58] in place, we can expect major advances in our knowledge of the mechanics of early human development.

Domes

Domes are curved, lumenized epithelial structures attached to a substrate [59,60] (Figure 2C,C′). They can be used to model naturally lumen-filled organs, such as the blastocyst or the otic vesicle, as well as diseased organs, such as the polycystic kidney with more control compared with the free-floating 3D spheres discussed above. Currently, dome generation success depends on cell type and relies on spontaneous cellular ion pumping.

In 1969, hemispherical blister-like structures were observed in MDCK monolayers [61]. These tissue domes form due to water influx basally, where the ion concentration is higher because of cell pumping, altering the osmotic pressure. Leveraging this phenomenon, the size and site of dome formation can be controlled by micropatterning ECM protein (fibronectin) on soft **polydimethylsiloxane** (PDMS) gels [59] to generate artificial domes with basal lumen formation due to localized detachment from the substrate. This synthetic system was used to show that the MDCK epithelium adapts to extreme tissue strains that develop in a dome by allowing heterogeneous cell strains. At high tissue strains, some cells start exhibiting superelastic properties due to cortical dilution, allowing them to accommodate up to tenfold increases in apical area. These large deformations do not damage the dome because of the intermediate filaments, which act as a safety belt. This mechanism identified in a synthetic system was later established *in vivo* during *Drosophila* gastrulation [62]. More recent studies also took advantage of closed-dome structures to map stresses on domes of different shapes [60] and built domes from human stem cells [7], with an elongated footprint to mimic the neural tube geometry. Here, stem cells seeded on rectangular patterns were covered with Matrigel and subsequently self-organized into a tissue bilayer. In time, a lumen opened between the layers, creating a tubular dome. Upon induction of neural cell fate by BMP4, a neural tube-like structure formed in the dome, surrounded by the domed non-neural ectoderm as *in vivo*. Here, the shape of the initial tissue affected the shape of the emerging neural tube. For example, a too-wide tissue footprint resulted in two parallel indenting regions, rather than one, indicating that strict control over initial geometry is essential for healthy development. This study demonstrates the power of *in vitro* morphogenesis to learn about

processes and tissues that are typically difficult to control, such as human or post-implantation tissues of other mammals.

A point to keep in mind while studying domed structures is the polarity of the dome (i.e., whether the lumen is on the basal or on the apical side of the tissue). Aside from the blastocyst, most *in vivo* luminal tissues have apical lumens. In addition to most signaling hubs being localized apically, the apical and basal sides of an epithelium also host different junctions, cytoskeletal, and cortical elements, endowing them different mechanical and mechanoresponsive properties [63]. Therefore, the same tissue with an apical or a basal lumen might require different luminal pressures, be differently pliable and respond differently to changes in shape (see 'Bending' section; Figure 1A') [5].

In the future, we expect to see the dome architecture leveraged to create more systems in which luminal pressure can be controlled, as well as advances in theoretical modeling that will enable mechanical characterization of domed structures with different geometries (e.g., rectangular and round combined) or thicker domes (larger lateral surfaces), more reminiscent of developing *in vivo* tissues.

Tubes

Tissue tubes can originate from all three germ layers and build the respiratory, vascular, lymphatic, urinary, reproductive, neural, and gastrointestinal systems. They are not only essential formations delivering products of most excretory tissues (e.g., pancreas, liver, and mammary) to their target location, but also the starting points of development for some organs (e.g., heart and neural tube). *In vivo* and *in vitro*, tube-building endothelial cells respond to mechanical properties of their environment. These include transcriptional responses to ECM stiffness [64] or responses to fluid flow. For example, endothelial cells align in the direction of flow-generated shear stress [65], but tend to migrate against the flow [66]. In the zebrafish dorsal aorta, cell extrusion is mechanoresponsive and increases under abnormally low blood flow [67].

Engineering long tubular systems is typically linked to elastomeric (PDMS) structures, either fixed microfluidic devices [25] (Figure 2D) or deformable tubular shells [68,69] (Figure 2E). Seeded cells line these channels, akin to *in vivo* lumen ensheathment [70]. As the resulting tissue tube takes the shape and size of the confinement, these substrate configurations allow control over tube geometry and size. For example, deformable alginate tubes (Figure 2E') [68] were used to control both tube diameter and its curvature. By tracking the rate at which epithelia detached from the tube walls, researchers were able to rank two cell lines by contractility, with MDCK cells exhibiting higher contractility compared with mammary gland epithelial J3B1A cells. However, preformed channels are not suitable for studies of lumen creation by more common mechanisms, such as cord hollowing or cavitation [71,72].

Critical advancements in our understanding of *de novo* lumen formation come from studying lumenization in organotypic cultures of spherical cysts (acini [73] and closed domes [74]; reviewed in [75]). When cysts of biliary epithelial cells are transferred from microwells into microfluidic channels, they open and line the channel to form tubular, partial bile duct-like structures [76]. To elongate a lumen in a formed tissue cord without breaking open a cyst, one can look for cues in vasculogenesis [i.e., the formation of the primary axial blood vessels, rather than the formation of higher order vessels (angiogenesis)]. In the zebrafish dorsal artery, lumens open up by a cord hollowing mechanism similar to lumens in cysts mentioned above, while, in mouse, two distinct cord-like tissues fuse, maintaining a lumen in between [77]. However, synthetic systems exploiting these mechanisms are still in their infancy. In a minimal system of

two hepatocyte cells in a microwell [78], the lumen between them elongates toward minimal tension, formed by anisotropies in integrin adhesion and, consequently, intercellular tension and osmotic pressure. Synthetic anisotropic protein patterns might also help to elongate lumens in larger cell groups. In another study reminiscent of cord hollowing, covering micropatterned colonies of stem cells with ECM induced the separation of apical surfaces and consequent lumen opening (see 'Domes' section [7]). It would be interesting to attempt to fuse multiple elongated domed lumens by targeted protein patterning, fluid flow, or barrier removal to extend tubular stem cell structures and potentially differentiate them.

A possible avenue to increase complexity by more elaborate shapes lies in building epithelial branches and networks of epithelial tubes. Factors that drive branch development depend on the tissue type and stage of network development and, consequently, the roles of mechanical factors here remain controversial [79]. Fluid flow is known to guide morphogenesis of lungs and kidneys [79–81], glands (reviewed in [82], and secondary vasculature (reviewed in [83]). In the lung, the pattern of the surrounding muscle drives branch patterning [84], whereas, in lung organoids, patterns are set by proliferative instabilities [85]. Synthetic systems investigating branching processes typically have a fixed network topology (reviewed in [86]). However, some use **matrix metalloprotease** (MMP)-degradable substrates, either natural or synthetic [87], to investigate network remodeling. Combined with biophysical tools, such as laser ablation, traction measurements, or optogenetics, synthetic branching systems can have the potential to not only identify forces that define network topology and function [88,89], but also characterize previously unreported structures.

Engineering tissue folding

Morphogenesis throughout the animal kingdom depends on correctly generating epithelial folds in more basic shapes, such as those discussed above. Folds are precursors (imaginal discs, vertebrate heart, or retina) or final functional structures (gyrencephalic brain or intestinal epithelium), but also appear as outgrowths in diseased states (pancreatic ductal cancer or colon polyps). Here, we discuss different approaches to engineer folds in elementary tissue shapes (Figure 3).

Scaffolding

Constant advances in microfabrication and material chemistry produced myriad biocompatible substrates (Box 2) that can be shaped [8,90–92], degraded [90], or 'programmed' [36,93–95] to have 3D folds. After seeding cells on the prefolded substrate (Figure 3A), the tissue assumes the shape of this scaffold (Figure 3A′). This allows studies of the effect of curvature on cell type localization, cell differentiation, cell migration or overall tissue patterning, a phenomenon collectively referred to as curvotaxis [96]. MDCK cells in monolayers grown on undulating hydrogels (Figure 3A″) are thinner on top of 'hills' and thicker in 'valleys' [36], independent of scaffold wavelength. They appear to sense curvature through cell thickness, tissue density, and nuclear shape and position, and respond by subsequent changes in the localization of YAP (lower in high density regions), expression of nuclear lamins, and proliferation rate. Cell localization within a migrating curved epithelial monolayer (leader versus midcluster), as well as the size of the cell cluster [96] and curvature magnitude [97] all affect F-actin and nuclear positioning, excluding both from highly convex regions [97], and longitudinal groove scaffolds help orient monolayer growth [97]. The intestinal epithelium also senses curvature. Intestinal crypt-like regions of organoids preferentially localize in indented regions of the scaffold, while differentiated villus cells cover finger-like protrusions of the substrate [90]. Even though the 3D geometry is not necessary for crypt and villus compartmentalization [39], the scaffolding results indicate that curvature helps maintain the fixed localization of intestinal compartments. Biologically more complex scaffolds were created from a mesenchyme-like tissue made of precisely localized mesenchymal cell clusters covered

Box 2. Homage to substrates

Mechanical properties of the tissue environment have a crucial role in guiding morphogenesis by affecting cell contractility, migration, division, death, extrusion, and differentiation. Given that substrates are in general easier to shape than are tissues both in 2D and 3D, harnessing properties of the diverse available substrates in projects of synthetic morphogenesis makes possible the generation of more controlled structures. Substrates used *in vitro* include natural and synthetic substrates, which offer differing levels of control. Natural substrates include those of animal origin, such as collagen or gelatin gels, commercial ECM extracts of mammalian tumors (Matrigel, Basement Membrane Extract, and Geltrex), and animal-free matrices (plant-based, Growdex; algal, alginate; and bacterial, hyaluronic acid). ECMs of animal origin contain natural biochemical cues and protein structures and can be degraded by cells. However, these properties are also problematic, because degradability means that the substrate shape cannot be well controlled, biochemical cues are present at inconsistent amounts, and matrices have complex or unknown mechanical properties. Reducing the complexity of mechanical properties of natural substrates, a preprint [144] reports controlling viscoelasticity independent of substrate stiffness using alginate. Natural matrix stiffness is typically low, 10–300 Pa, which limits studies of durotaxis and production of stable structures. Increasing stiffness also usually implies increasing protein and growth factor concertation. However, collagen gels can be made stiffer, and their compressive modulus can be decoupled from protein content, for example by glycation [145] (reviewed in [146]) and its stiffness can increase up to 6 kPa when methacrylated (**gelatin methacryloyl**; GelMA).

Synthetic substrates mitigate the complexity of natural substrates and include glass, plastic, PAA, soft PDMS, NuSil PDMS, PEG, **polyethylene glycol diacrylate-acrylic acid** (PEGDA-AA), PEG with functional additions and **Norland Optical Adhesive** (NOA). They have also been adapted to be artificially degradable and deformable [147]. To control tissue size and shape, and cell adhesion, (synthetic) substrates are usually functionalized. Their surface can be micropatterned, which implies that ECM proteins (collagens, laminins, fibronectin, etc., depending on cell type) are bound to a (2D) substrate in a defined spatial pattern and size, such as circular, triangular, square, or rings. Proteins can be patterned using physical transfers from 3D stamps that carry the pattern (μ-contact printing) or through contactless methods that expose protein-binding molecules only on the pattern [UV through patterned masks or digitally guided, maskless light exposure (PRIMO)]. Contactless patterning systems also allow creation of protein gradients, while multiprotein patterns can, in principle, be generated by both approaches. However, protocols for such more complex patterning are still not widely used due to the extensive optimization required for different proteins and substrates. In addition to surface functionalization, substrate bulk can be functionalized with coated beads that serve as a growth factor/signaling source and with micro- and nanofluorospheres to track substrate deformation and measure cell–substrate traction forces.

by ECM [93]. The mesenchymal clusters compacted the ECM and introduced complex folds in the epithelium seeded on top, akin to folds in the intestine or avian skin.

Aside from folding the tissue by the substrate guiding its shape, folds can be generated by exploiting the tissue-intrinsic forces to drive passive buckling (Figure 3B) or active bending (Figure 3C; reviewed in [98,99]), which we discuss below.

Buckling

Buckling is a passive deformation normal to the tissue plane that results from lateral compression (in plane of the epithelium) occurring, for example, during confined growth of a tissue [100]. *In vivo*, buckling was suggested to drive specific stages of morphogenesis of teeth (germ invagination [101]), brain (reviewed in [102], although the mechanism is controversial), lung [85], and intestine (tube looping and villus formation [103]), forming stable folds by releasing built-up compression (Figure 3B,B′). Synthetic buckling was achieved with MDCK monolayers grown inside a spherical confinement [24]. The tissue buckled basally under lateral compression from proliferation, allowing the authors to report the buckling pressure of an epithelial monolayer to be ~100 Pa. Such a system allows testing of different confinement geometries (see 'Tubes' section), but does not allow precise control of compressive force. To investigate how epithelia respond to compressive strain without effects of the substrate, researchers work with suspended tissues [104]. In 2020, a suspended epithelium was used to identify ~–35% strain as the MDCK buckling threshold [105], which depends on tissue elasticity and prestrain (Figure 3B″). Below this threshold, epithelia were able to accommodate the applied compression without buckling. A suspended tissue is a powerful technique but it can be applied only to cell types that form strong cell–cell junctions. In addition, to study epithelial invagination (i.e., buckling from the

apical surface inwards) a pressure-based system (see 'Bending' section [5]) could be used to assess mechanical differences depending on fold direction, although it would need to be adapted to exert buckling-inducing forces.

Tissue thickness affects the mechanical properties of an epithelium and buckling is more common in thin structures, as many adult epithelia are. However, many developing tissues, such as the vertebrate retina, brain, or insect imaginal discs, are thick, pseudostratified epithelia (>20 μm apicobasal axis [106]) and require complementary destabilizing mechanisms to induce a bend that will localize buckling. These mechanisms include local apical, basal, or lateral cell constriction (see 'Bending' section), mitotic cell rounding [107], and cell death [108,109]. Currently, it is difficult to control buckling of thick tissues *in vitro*, as it is to grow such tissues in the first place. *In vitro* systems that self-organize into pseudostratified compartments, such as the open-lumen intestinal organoid with its pseudostratified crypt, might prove useful to study physics of more complex buckling phenomena.

Bending

To examine the effects of curvature change on the epithelium, pressure-based doming systems can be used [5]. An epithelial monolayer is grown on a thin elastic membrane suspended over a microfluidic channel. By applying positive or negative pressure in the channel, the epithelium is pulled inward (smaller apical surface) or bulges outward (smaller basal surface), thus assuming opposite curvatures. These different configurations trigger different propagations of Ca^{2+} waves and gene expression at the fold boundary, through different mechanical stresses that cells experience with varying shapes.

However, the introduction of localized bends *in vivo* is a process typically driven by active changes in cell shape through apical [110], basal [111], or lateral [108,112,113] constriction (Figure 3C). Such processes *in vitro* can be driven by both tissue self-organization and extrinsic control. Open-lumen intestinal organoids, mentioned above, were shown to indent their crypts on soft substrates (<1.5 kPa, [39]) through self-organized apical constriction of stem cells. The same tissue was grown in light-degradable **polyethylene glycol** (PEG) substrates [90] and the substrate was locally softened, allowing the crypts to invaginate into the substrate in these softer regions. To manipulate such active tissue bending *in vivo,* studies genetically interfered with relevant transcription factors [114,115], or used laser ablation [116] or optogenetics [117]. *In vitro*, the CRY2/CIBN light dimerizer system was used in MDCK cells to activate RhoA with subcellular resolution using blue light [22]. Recently, OptoShroom3 was developed [118] (Figure 3C″) to allow light-induced constriction specifically of the apical cell surface in mammalian cells. With these tools, single cell-shape changes or tissue-wide folds can be introduced depending on the number of activated cells. Future studies should also look away from the apical surface and to the morphogenetic potential of lateral and basal cell contraction to understand the mechanics of tissue bending and buckling.

Harnessing cell dynamics

In the previous sections, we discussed strategies to engineer elementary shapes and processes that build living tissues. Here, we describe how the ceaseless out-of-equilibrium dynamics of living cells, which direct natural morphogenetic processes, can be exploited during synthetic morphogenesis.

Topological defects

In active systems, orientation and topological defects entail specific mechanical patterns. Defect sites were recently identified as powerful localizers of morphogenetic processes, namely tissue

organization in the mammalian liver [119] or body axis establishment in hydra [120] *in vivo* and 3D outgrowth from a monolayer *in vitro* [121,122]. Nematic order and topological defects may arise from supracellular actin cable orientation [120] or cell shape orientation [18,119,121,122]. *In vitro*, topological defects can be controlled by imposing geometrical/topological constraints (e.g., star [18] or disk [121]). It was shown in star-shaped tissue monolayers [18] that MDCK cell extrusion increased at +1/2 defects. By contrast, neural progenitor cells accumulated and formed a 3D mound at +1/2 defects and escaped from –1/2 defects [122] (Figure 4A). These differences might be due to cell-type specifics, such as the strength of cell adhesion. The same mechanisms might have a role *in vivo*, and guide morphogenesis in various systems. Overall, topological defects not only shape tissues *in vivo*, but also help to predict and execute controlled morphogenetic processes *in vitro*.

Cell turnover

Cell extrusion and division are tightly regulated to maintain mechanical stress distribution in a tissue during morphogenesis [123]. During synthetic morphogenesis, proliferation and extrusion can also be exploited as a building mechanism to, for example, induce tissue compression or generate tissue flows. However, they also need to be controlled or (pharmacologically) slowed down, if necessary, because cell turnover might destabilize the synthetic structure or create

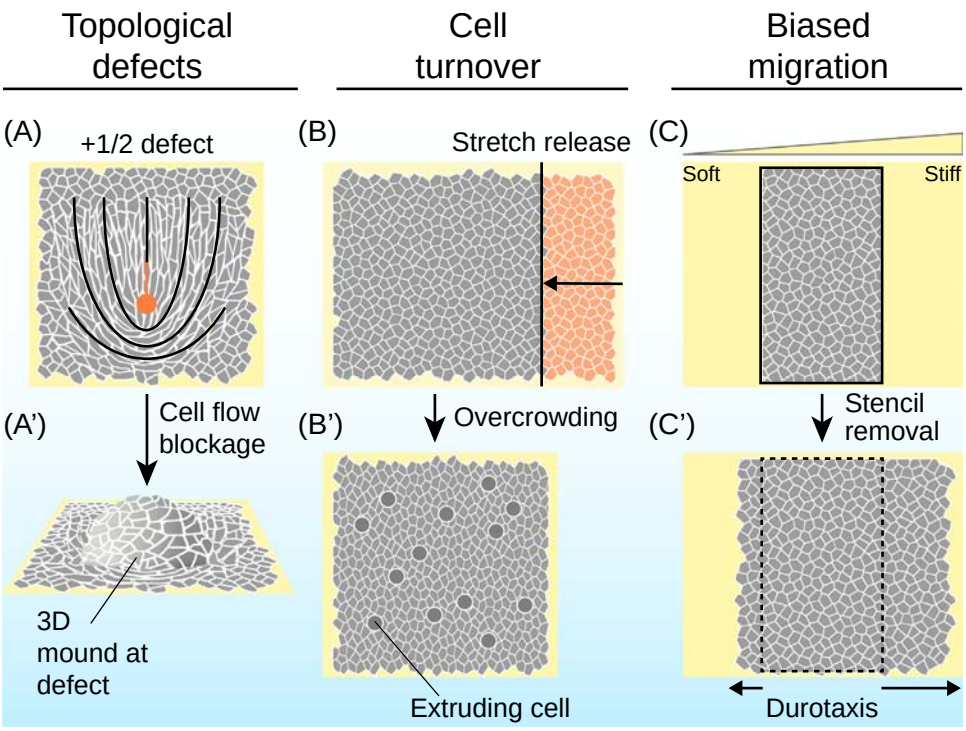


Figure 4. Controlling cell dynamics. (A,A') Sites of topological defects localize mechanical patterns that can drive morphogenetic processes. (A) +/1/2 defect in a monolayer of mouse neural progenitor cells, which blocks cell flow at the front point of the defect; (A') consequent formation of a 3D mound at the defect site. (B,B') Cell turnover can be controlled in synthetic systems. (B) Stretching MDCK monolayers by 28% by stretching the underlying membrane substrate. (B') Stretch release induces overcrowding in the monolayer, which peaks 0.5 h after release. Crowding induces cell extrusion to maintain homeostatic cell density. Extrusion rate peaks 2 h after stretch release. (C,C') Cell migration can be controlled by exploiting mechanical cues for migration, such as substrate stiffness. (C) Cells were grown on polyacrylamide (PAA) substrates with a gradient of stiffness [132], limited by a 500-μm stencil. (C') After stencil removal, cells migrated preferentially toward stiffer regions of the substrate, displaying positive durotaxis. Adapted from [122] (A,A') and [23] (B,B').

luminal obstruction by agglomerations of extruded cells. Studies have already exploited proliferation as a morphogenetic mechanism in *in vitro* systems (e.g., [24]). Simple 2D setups were sufficient to suggest that outcomes depend on cell type. For example, in confined round monolayers, proliferating myoblasts form 3D cell accumulations in the center of the monolayer island [121], while MDCK cells accumulate on the monolayer edge [124], creating a 3D cord-like structure with collective polarity. It is unclear how these different behaviors arise from different levels of cell–cell adhesion, traction, friction, and contractility among different cell types.

Localized or differential proliferation drives many morphogenetic processes *in vivo*, such as the development of the vertebrate tooth or heart, or *Drosophila* wing disc [125–127]. As a mechanoresponsive feature, proliferation could be also localized *in vitro* by controlling tissue shape [19], locally stretching/compressing the tissue on stretch systems [23] (Figure 4B), light-responsive hydrogels [128] or ferrogels [129], mixing clones that grow at different rates [130], or altering mechanical feedback that controls proliferation [130].

Compared with proliferation, cell extrusion has attracted less attention in synthetic systems but also holds significant potential to guide folding or control general tissue stresses, for example by locally increasing the apicobasal force in the epithelium [108,109]. It can be mechanically triggered and localized similar to cell proliferation but with the opposite effect of force application, and with the additional option of inducing extrusion through cell death, for example by laser ablation or ultraviolet (UV) exposure. Together, control over cell proliferation and extrusion holds more potential than synthetic morphogenesis has exploited thus far.

Cell migration

In a system of guided morphogenesis, cell migration can be both a desired [e.g., gap closure, **epithelial–mesenchymal transition** (EMT)] and undesired (destabilizing the structure or introducing defects) behavior. There are several ways in which mechanics can control migration. Most cell types (primer in [131]) migrate toward stiffer substrates (positive durotaxis; Figure 4C [132]). However, some cell types (e.g., axons of retinal ganglion cells in *Xenopus*, U251-MG glioma cells [148]) follow different gradients and move towards the stiffness where they can generate maximal tractions [148]; thus, the stiffness of the synthetic environment should be designed with the cell type in mind. The same holds true for haptotaxis of adherent cells, in which fibroblasts migrate toward regions with higher protein density more efficiently than do mesenchymal stem cells [133]. Of note, ameboid cells, such as leukocytes, were shown to follow opposite haptotactic gradients depending on the integrin ($\alpha4\beta1$ or $\alpha_L\beta_4$) used in their migration [134], opening a potential avenue for genetically altering epithelial cell migration. Migration of some cell types can also be controlled by substrate curvature (curvotaxis [96]), as well as fluid flow. In *in vitro* tubes of endothelial cells, cell migration would be necessary to grow and fuse tubes, and the direction of migration could be controlled by fluid flow direction [66] (reviewed in [82]). In many cases, factors mentioned above also affect cell fate, a point to be considered especially while building structures of stem cells, where stemness-promoting factors can be used to mitigate unwanted differentiation and any associated mechanical and behavioral changes. In more recent developments, direct laser writing was applied on a synthetic substrate to create custom surfaces for endothelial cell migration [135] and optogenetics was used to direct cell migration of specific cells [136,137]. During synthetic morphogenesis, cell speed could be finely controlled by combining the aforementioned approaches, such as synthesizing substrates with different gradients of stiffness and ECM density.

Concluding remarks

During development and disease, morphogenesis implies a combination of multiple shapes, such as tubes and buds [138], and synthetic systems should be able to recapitulate these features

Outstanding questions

What are the limits of complexity that synthetic morphogenesis can rationally engineer?

How can mechanical stresses be mapped and controlled in synthetic tissue structures?

Which functional features depend on a 3D configuration, and which can be recapitulated in 2D and why?

Can synthetic morphogenesis capture mechanochemical redundancies present *in vivo*?

What is the minimal set of physical variables that need to be controlled to engineer multicellular morphogenetic processes?

How can we combine synthetic generation of different shapes, such as tubes and spheres, or branches and buds?

Can we predict the mechanical stability of synthetic living structures based on cell type and shape?

As complexity increases, what type of theoretical mechanical model will be needed to synthesize morphogenetic processes?

Can we build shapes that do not occur naturally in 3D, perhaps with supernatural functionalities?

while maintaining control and accessibility. We expect the most productive future avenues will address the outstanding challenges by incorporating next-level ideas including: (i) building more elaborate shapes and combining different shapes; (ii) building shapes from multiple cell types and from different species (chimeras); (iii) simultaneously controlling multiple cell behaviors, such as contractility, adhesion, cell localization, cell differentiation, tissue growth rate, or lumen formation; (iv) controlling cell behavior in a cell type-specific manner; and (v) rather than building by assembling, building by predictable collapse of 3D structures (see Outstanding questions).

To highlight our engineering perspective on synthetic morphogenesis in this review, we grouped morphogenesis in discrete shapes and processes and discussed the experimental and mechanical aspect of building such elementary blocks. For an overview of top-down and bottom-up techniques to alter extracellular and cell-intrinsic mechanical properties in tissue engineering, we refer the reader to an excellent recent review [139]. For an open-source tool to compute traction forces, see [140] and for an in-depth overview of the latest developments to measure mechanical stress in tissues in 2D and 3D, see [141].

Tissues *in vivo* depend on complex but precise mechanical and biochemical signals. Minimal systems, such as epithelial monolayers on synthetic substrates, allow us to narrow down the determinants of shape and function of organs. From the point of view of morphogenetic tissue mechanics, adding complexity to these systems is a clear aim, but should not be done at the expense of control and accessibility. Therefore, we encourage the development of mechanically controllable systems. By building from the bottom-up, we will slowly learn which cues are essential for which tissue and which living form.

Acknowledgements

We thank the members of the Trepat, Roca-Cusachs, and Arroyo laboratories for their discussions and support. This work was supported by: European Molecular Biology Organization (ALTF-1169 to M.M.), Generalitat de Catalunya (Agaur, Spain, SGR-2017-01602 to X.T.); Spanish Ministry for Science and Innovation MICCINN/FEDER (Spain, PGC2018-099645-B-I00 to X.T.); European Research Council (Adv-883739 to X.T.), Fundació la Marató de TV3 (Spain, project 201903-30-31-32 to X.T.); IBEC, IRB, and CIMNE are is a recipient of the Severo Ochoa Award of Excellence from the MINECO (Spain); La Caixa Foundation (Spain, LCF/PR/HR20/52400004).

Declaration of interests

The authors declare no competing interests.

References

1. Sasai, Y. (2013) Cytosystems dynamics in self-organization of tissue architecture. *Nature* 493, 318–326
2. Guye, P. *et al.* (2016) Genetically engineering self-organization of human pluripotent stem cells into a liver bud-like tissue using Gata6. *Nat. Commun.* 7, 1–12
3. Johnson, H.E. *et al.* (2020) Optogenetic rescue of a patterning mutant. *Curr. Biol.* 30, 3414–3424
4. Muncie, J.M. *et al.* (2020) Mechanical tension promotes formation of gastrulation-like nodes and patterns mesoderm specification in human embryonic stem cells. *Dev. Cell* 55, 679–694
5. Blonski, S. *et al.* (2021) Direction of epithelial folding defines impact of mechanical forces on epithelial state. *Dev. Cell* 56, 3222–3234
6. Warmflash, A. *et al.* (2014) A method to recapitulate early embryonic spatial patterning in human embryonic stem cells. *Nat. Methods* 11, 847–854
7. Karzbrun, E. *et al.* (2021) Human neural tube morphogenesis *in vitro* by geometric constraints. *Nat.* 599, 268–272
8. Huang, C.-K. *et al.* (2022) Surface curvature and basal hydraulic stress induce spatial bias in cell extrusion. *bioRxiv* Published online May 29, 2022. https://doi.org/10.1101/2022.04.01.486717
9. Ramadan, Q. and Zourob, M. (2021) 3D bioprinting at the frontier of regenerative medicine, pharmaceutical, and food industries. *Front. Med. Technol.* 2, 607648
10. Huh, D. *et al.* (2011) From 3D cell culture to organs-on-chips. *Trends Cell Biol.* 21, 745–754
11. Ronaldson-Bouchard, K. and Vunjak-Novakovic, G. (2018) Organs-on-a-chip: a fast track for engineered human tissues in drug development. *Cell Stem Cell* 22, 310–324
12. Tajeddin, A. and Mustafaoglu, N. (2021) Design and fabrication of organ-on-chips: promises and challenges. *Micromachines* 12, 1443
13. Ingber, D.E. (2022) Human organs-on-chips for disease modelling, drug development and personalized medicine. *Nat. Rev. Genet.* Published online March 25, 2022. https://doi.org/10.1038/S41576-022-00466-9
14. Patwari, P. and Lee, R.T. (2008) Mechanical control of tissue morphogenesis. *Circ. Res.* 103, 234–243
15. Goodwin, K. and Nelson, C.M. (2021) Mechanics of development. *Dev. Cell* 56, 240–250
16. Winter, G.D. and Simpson, B.J. (1969) Heterotopic bone formed in a synthetic sponge in the skin of young pigs. *Nature* 223, 88–90

17. Junquera, P. (1984) Oogenesis in a paedogenetic dipteran insect under normal conditions and after experimental elimination of the follicular epithelium: an ultrastructural study. *Wilhelm Rouxs Arch. Dev. Biol.* 193, 197–204
18. Saw, T.B. *et al.* (2017) Topological defects in epithelia govern cell death and extrusion. *Nature* 544, 212–216
19. Nelson, C.M. *et al.* (2005) Emergent patterns of growth controlled by multicellular form and mechanics. *Proc. Natl. Acad. Sci. U. S. A.* 102, 11594–11599
20. Benham-Pyle, B.W. *et al.* (2015) Mechanical strain induces E-cadherin-dependent Yap1 and β-catenin activation to drive cell cycle entry. *Science (80-.)* 348, 1024–1027
21. Streichan, S.J. *et al.* (2014) Spatial constraints control cell proliferation in tissues. *Proc. Natl. Acad. Sci. U. S. A.* 111, 5586–5591
22. Valon, L. *et al.* (2017) Optogenetic control of cellular forces and mechanotransduction. *Nat. Commun.* 8, 14396
23. Eisenhoffer, G.T. *et al.* (2012) Crowding induces live cell extrusion to maintain homeostatic cell numbers in epithelia. *Nature* 484, 546–549
24. Trushko, A. *et al.* (2020) Buckling of an epithelium growing under spherical confinement. *Dev. Cell* 54, 655–668
25. Li, X. *et al.* (2015) *In vitro* recapitulation of functional microvessels for the study of endothelial shear response, nitric oxide and [Ca2+]i. *PLoS ONE* 10, e0126797
26. Shin, W. and Kim, H.J. (2022) 3D *in vitro* morphogenesis of human intestinal epithelium in a gut-on-a-chip or a hybrid chip with a cell culture insert. *Nat. Protoc.* 17, 910–939
27. Morgani, S.M. *et al.* (2018) Micropattern differentiation of mouse pluripotent stem cells recapitulates embryo regionalized cell fate patterning. *Elife* 7, e32839
28. Anlas, K. and Trivedi, V. (2021) Studying evolution of the primary body axis *in vivo* and *in vitro*. *Elife* 10, e69066
29. Moris, N. *et al.* (2020) Experimental embryology of gastrulation: pluripotent stem cells as a new model system. *Curr. Opin. Genet. Dev.* 64, 78–83
30. Nelson, C.M. *et al.* (2017) Microfluidic chest cavities reveal that transmural pressure controls the rate of lung development. *Development* 144, 4328–4335
31. Blin, G. (2021) Quantitative developmental biology *in vitro* using micropatterning. *Development* 148, dev186387
32. Van Den Brink, S.C. *et al.* (2014) Symmetry breaking, germ layer specification and axial organisation in aggregates of mouse embryonic stem cells. *Development* 141, 4231–4242
33. Deglincerti, A. *et al.* (2016) Self-organization of human embryonic stem cells on micropatterns. *Nat. Protoc.* 11, 2223–2232
34. Tewary, M. *et al.* (2019) High-throughput micropatterning platform reveals Nodal-dependent bisection of peri-gastrulation-associated versus preneurulation-associated fate patterning. *PLoS Biol.* 17, e3000081
35. Britton, G. *et al.* (2019) A novel self-organizing embryonic stem cell system reveals signaling logic underlying the patterning of human ectoderm. *Dev.* 146, dev179093
36. Luciano, M. *et al.* (2021) Cell monolayers sense curvature by exploiting active mechanics and nuclear mechanoadaptation. *Nat. Phys.* 17, 1382–1390
37. Knight, G.T. *et al.* (2018) Engineering induction of singular neural rosette emergence within hPSC-derived tissues. *Elife* 7, e37549
38. Thorne, C.A. *et al.* (2018) Enteroid monolayers reveal an autonomous WNT and BMP circuit controlling intestinal epithelial growth and organization. *Dev. Cell* 44, 624–633
39. Pérez-González, C. *et al.* (2021) Mechanical compartmentalization of the intestinal organoid enables crypt folding and collective cell migration. *Nat. Cell Biol.* 23, 745
40. He, S. *et al.* (2021) Stiffness regulates intestinal stem cell fate. *bioRxiv* Published online March 16, 2021. https://doi.org/10.1101/2021.03.15.435410
41. Alessandri, K. *et al.* (2016) A 3D printed microfluidic device for production of functionalized hydrogel microcapsules for culture and differentiation of human neuronal stem cells (hNSC). *Lab Chip* 16, 1593–1604
42. Natsiou, D. *et al.* (2017) Generation of spheres from dental epithelial stem cells. *Front. Physiol.* 8, 7
43. Pastrana, E. *et al.* (2011) Eyes wide open: a critical review of sphere-formation as an assay for stem cells. *Cell Stem Cell* 8, 486
44. Weiswald, L.B. *et al.* (2015) Spherical cancer models in tumor biology. *Neoplasia* 17, 1
45. Gjorevski, N. *et al.* (2016) Designer matrices for intestinal stem cell and organoid culture. *Nature* 539, 560–564
46. Rivron, N.C. *et al.* (2018) Blastocyst-like structures generated solely from stem cells. *Nature* 557, 106–111
47. Sozen, B. *et al.* (2019) Self-organization of mouse stem cells into an extended potential blastoid. *Dev. Cell* 51, 698–712
48. Kime, C. *et al.* (2019) Induced 2C expression and implantation-competent blastocyst-like cysts from primed pluripotent stem cells. *Stem Cell Reports* 13, 485
49. Liu, X. *et al.* (2021) Modelling human blastocysts by reprogramming fibroblasts into iBlastoids. *Nature* 591, 627–632
50. Yu, L. *et al.* (2021) Blastocyst-like structures generated from human pluripotent stem cells. *Nature* 591, 620–626
51. Sozen, B. *et al.* (2021) Reconstructing aspects of human embryogenesis with pluripotent stem cells. *Nat. Commun.* 12, 1–13
52. Gupta, A. *et al.* (2021) Bioengineering *in vitro* models of embryonic development. *Stem Cell Reports* 16, 1104
53. Shahbazi, M.N. *et al.* (2019) Self-organization of stem cells into embryos: a window on early mammalian development. *Science (80-.)* 364, 948–951
54. Simunovic, M. and Brivanlou, A.H. (2017) Embryoids, organoids and gastruloids: new approaches to understanding embryogenesis. *Development* 144, 976–985
55. Kagawa, H. *et al.* (2021) Human blastoids model blastocyst development and implantation. *Nature* 601, 600–605
56. Zheng, Y. *et al.* (2020) A microfluidics-based stem cell model of early post-implantation human development. *Nat. Protoc.* 16, 309–326
57. Chan, C.J. *et al.* (2019) Hydraulic control of mammalian embryo size and cell fate. *Nature* 571, 112–116
58. Dumortier, J.G. *et al.* (2019) Hydraulic fracturing and active coarsening position the lumen of the mouse blastocyst. *Science (80-.)* 365, 465–468
59. Latorre, E. *et al.* (2018) Active superelasticity in three-dimensional epithelia of controlled shape. *Nature* 563, 203–208
60. Marín-Llauradó, A. *et al.* (2022) Mapping mechanical stress in curved epithelia of designed size and shape. *bioRxiv* Published online May 4, 2022. https://doi.org/10.1101/2022.05.03.490382
61. Leighton, J. *et al.* (1969) Secretory activity and oncogenicity of a cell line (MDCK) Derived from canine kidney. *Science (80-.)* 163, 472–473
62. Bhide, S. *et al.* (2021) Mechanical competition alters the cellular interpretation of an endogenous genetic program. *J. Cell Biol.* 220, e202104107
63. Badugu, A. and Käch, A. (2020) Independent apical and basal mechanical systems determine cell and tissue shape in the *Drosophila* wing disc. *bioRxiv*. Published online April 12, 2020. https://doi.org/10.1101/2020.04.10.036152
64. Frye, M. *et al.* (2018) Matrix stiffness controls lymphatic vessel formation through regulation of a GATA2-dependent transcriptional program. *Nat. Commun.* 9, 1–16
65. Levesque, M.J. and Nerem, R.M. (1985) The elongation and orientation of cultured endothelial cells in response to shear stress. *J. Biomech. Eng.* 107, 341–347
66. Ostrowski, M.A. *et al.* (2014) Microvascular endothelial cells migrate upstream and align against the shear stress field created by impinging flow. *Biophys. J.* 106, 366–374
67. Campinho, P. *et al.* (2020) Blood flow limits endothelial cell extrusion in the zebrafish dorsal aorta. *Cell Rep.* 31, 107505
68. Maechler, F.A. *et al.* (2019) Curvature-dependent constraints drive remodeling of epithelia. *J. Cell Sci.* 132, jcs222372
69. Zhang, W. *et al.* (2016) Elastomeric free-form blood vessels for interconnecting organs on chip systems. *Lab Chip* 16, 1579–1586
70. Helker, C.S.M. *et al.* (2013) The zebrafish common cardinal veins develop by a novel mechanism: lumen ensheathment. *Development* 140, 2776–2786

71. Hogan, B.M. and Schulte-Merker, S. (2017) How to plumb a pisces: understanding vascular development and disease using zebrafish embryos. *Dev. Cell* 42, 567–583
72. Andrew, D.J. and Ewald, A.J. (2010) Morphogenesis of epithelial tubes: Insights into tube formation, elongation and elaboration. *Dev. Biol.* 341, 34
73. Bryant, D.M. *et al.* (2014) A molecular switch for the orientation of epithelial cell polarization. *Dev. Cell* 31, 171
74. Rodríguez-Fraticelli, A.E. *et al.* (2012) Cell confinement controls centrosome positioning and lumen initiation during epithelial morphogenesis. *J. Cell Biol.* 198, 1011
75. Debnath, J. and Brugge, J.S. (2005) Modelling glandular epithelial cancers in three-dimensional cultures. *Nat. Rev. Cancer* 5, 675–688
76. Rizki-Safitri, A. *et al.* (2018) Efficient functional cyst formation of biliary epithelial cells using microwells for potential bile duct organisation *in vitro*. *Sci. Reports* 8, 1–11
77. Strilić, B. *et al.* (2009) The molecular basis of vascular lumen formation in the developing mouse aorta. *Dev. Cell* 17, 505–515
78. Li, Q. *et al.* (2016) Extracellular matrix scaffolding guides lumen elongation by inducing anisotropic intercellular mechanical tension. *Nat. Cell Biol.* 18, 311–318
79. Lang, C. *et al.* (2021) Organ-specific branching morphogenesis. *Front. Cell Dev. Biol.* 9, 1380
80. Palmer, M.A. *et al.* (2021) Stress ball morphogenesis: how the lizard builds its lung. *Sci. Adv.* 7, eabk0161
81. Unbekandt, M. *et al.* (2008) Tracheal occlusion increases the rate of epithelial branching of embryonic mouse lung via the FGF10-FGFR2b-Sprouty2 pathway. *Mech. Dev.* 125, 314
82. Campinho, P. *et al.* (2020) Blood flow forces in shaping the vascular system: a focus on endothelial cell behavior. *Front. Physiol.* 11, 552
83. Navis, A. and Nelson, C.M. (2016) Pulling together: tissue-generated forces that drive lumen morphogenesis. *Semin. Cell Dev. Biol.* 55, 139–147
84. Goodwin, K. *et al.* (2019) Smooth muscle differentiation shapes domain branches during mouse lung development. *Dev.* 146, dev181172
85. Varner, V.D. *et al.* (2015) Mechanically patterning the embryonic airway epithelium. *Proc. Natl. Acad. Sci. U. S. A.* 112, 9230–9235
86. Costa, L. *et al.* (2020) Microfluidics for angiogenesis research. *Adv. Exp. Med. Biol.* 1230, 97–119
87. Zanotelli, M.R. *et al.* (2016) Stable engineered vascular networks from human induced pluripotent stem cell-derived endothelial cells cultured in synthetic hydrogels. *Acta Biomater.* 35, 32–41
88. Goodwin, K. and Nelson, C.M. (2020) Branching morphogenesis. *Development* 147, dev184499
89. Vaeyens, M.M. *et al.* (2020) Matrix deformations around angiogenic sprouts correlate to sprout dynamics and suggest pulling activity. *Angiogenesis* 23, 315–324
90. Gjorevski, N. *et al.* (2022) Tissue geometry drives deterministic organoid patterning. *Science (80-.)* 375, eaaw9021
91. Altay, G. *et al.* (2022) Modelling biochemical gradients *in vitro* to control cell compartmentalization in a micro-engineered 3D model of the intestinal epithelium. *bioRxiv* Published online April 1, 2022. https://doi.org/10.1101/2021.12.13.472418
92. Altay, G. *et al.* (2020) Imaging the cell morphological response to 3D topography and curvature in engineered intestinal tissues. *Front. Bioeng. Biotechnol.* 8, 294
93. Hughes, A.J. *et al.* (2018) Engineered tissue folding by mechanical compaction of the mesenchyme. *Dev. Cell* 44, 165–178
94. Chen, T. *et al.* (2018) Combining 3D printing with electrospinning for rapid response and enhanced designability of hydrogel actuators. *Adv. Funct. Mater.* 28, 1800514
95. Kouroupis, A.P. and Nelson, C.M. (2018) Modeling branching morphogenesis using materials with programmable mechanical instabilities. *Curr. Opin. Biomed. Eng.* 6, 66–73
96. Pieuchot, L. *et al.* (2018) Curvotaxis directs cell migration through cell-scale curvature landscapes. *Nat. Commun.* 9, 1–13
97. Rougerie, P. *et al.* (2020) Topographical curvature is sufficient to control epithelium elongation. *Sci. Rep.* 10, 14784
98. Tozluo lu, M. and Mao, Y. (2020) On folding morphogenesis, a mechanical problem. *Philos. Trans. R. Soc. B Biol. Sci.* 375, 20190564
99. Pearl, E.J. *et al.* (2017) Cellular systems for epithelial invagination. *Philos. Trans. R. Soc. B Biol. Sci.* 372, 20150526
100. Nelson, C.M. (2016) On buckling morphogenesis. *J. Biomech. Eng.* 138, 0210051
101. Takigawa-Imamura, H. *et al.* (2015) Tooth germ invagination from cell–cell interaction: working hypothesis on mechanical instability. *J. Theor. Biol.* 382, 284–291
102. Garcia, K.E. *et al.* (2018) Mechanics of cortical folding: stress, growth and stability. *Philos. Trans. R. Soc. B Biol. Sci.* 373, 20170321
103. Shyer, A.E. *et al.* (2013) Villification: how the gut gets its villi. *Science (80-.)* 342, 212–218
104. Harris, A.R. *et al.* (2013) Generating suspended cell monolayers for mechanobiological studies. *Nat. Protoc.* 8, 2516–2530
105. Wyatt, T.P.J. *et al.* (2020) Actomyosin controls planarity and folding of epithelia in response to compression. *Nat. Mater.* 19, 109–117
106. Strzyz, P.J. *et al.* (2016) Heterogeneity, cell biology and tissue mechanics of pseudostratified epithelia: coordination of cell divisions and growth in tightly packed tissues. *Int. Rev. Cell Mol. Biol.* 325, 89–118
107. Kondo, T. and Hayashi, S. (2013) Mitotic cell rounding accelerates epithelial invagination. *Nature* 494, 125–129
108. Monier, B. *et al.* (2015) Apico-basal forces exerted by apoptotic cells drive epithelium folding. *Nature* 518, 245–248
109. Roellig, D. *et al.* (2022) Force-generating apoptotic cells orchestrate avian neural tube bending. *Dev. Cell* 57, 707–718
110. He, B. *et al.* (2014) Apical constriction drives tissue-scale hydrodynamic flow to mediate cell elongation. *Nature* 508, 392–396
111. Sidhaye, J. and Norden, C. (2017) Concerted action of neuroepithelial basal shrinkage and active epithelial migration ensures efficient optic cup morphogenesis. *Elife* 6, e22689
112. Sui, L. and Dahmann, C. (2020) Increased lateral tension is sufficient for epithelial folding in *Drosophila*. *Development* 147, dev194316
113. Gracia, M. *et al.* (2019) Mechanical impact of epithelial–mesenchymal transition on epithelial morphogenesis in *Drosophila*. *Nat. Commun.* 10, 2951
114. Córdoba, S. and Estella, C. (2018) The transcription factor Dysfusion promotes fold and joint morphogenesis through regulation of Rho1. *PLoS Genet.* 14, e1007584
115. Leptin, M. (1991) twist and snail as positive and negative regulators during *Drosophila* mesoderm development. *Genes Dev.* 5, 1568–1576
116. Guo, H. *et al.* (2022) Optogenetic inhibition of actomyosin reveals mechanical bistability of the mesoderm epithelium during *Drosophila* mesoderm invagination. *Elife* 11, e69082
117. De Renzis, S. (2020) Morphogenesis: guiding embryonic development with light. *Curr. Biol.* 30, R998–R1001
118. Martínez-Ara, G. *et al.* (2021) Optogenetic control of apical constriction induces synthetic morphogenesis in mammalian tissues. *bioRxiv* Published online April 26, 2022. https://doi.org/10.1101/2021.04.20.440475
119. Morales-Navarrete, H. *et al.* (2019) Liquid-crystal organization of liver tissue. *Elife* 8, e44860
120. Maroudas-Sacks, Y. *et al.* (2020) Topological defects in the nematic order of actin fibres as organization centres of Hydra morphogenesis. *Nat. Phys.* 17, 251–259
121. Guillamat, P. *et al.* (2022) Integer topological defects organize stresses driving tissue morphogenesis. *Nat. Mater.* 21, 588–597
122. Kawaguchi, K. *et al.* (2017) Topological defects control collective dynamics in neural progenitor cell cultures. *Nature* 545, 327–331
123. Schaefer, M. *et al.* (2000) A protein complex containing Inscuteable and the Gα-binding protein Pins orients asymmetric cell divisions in Drosophila. *Curr. Biol.* 10, 353–362
124. Deforet, M. *et al.* (2014) Emergence of collective modes and tri-dimensional structures from epithelial confinement. *Nat. Commun.* 5, 3747
125. Marin-Riera, M. *et al.* (2018) Differential tissue growth and cell adhesion alone drive early tooth morphogenesis: an ex vivo and in silico study. *PLoS Comput. Biol.* 14, e1005981

126. de Boer, B.A. *et al.* (2012) Growth of the developing mouse heart: an interactive qualitative and quantitative 3D atlas. *Dev. Biol.* 368, 203–213
127. Mao, Y. *et al.* (2013) Differential proliferation rates generate patterns of mechanical tension that orient tissue growth. *EMBO J.* 32, 2790
128. Takashima, Y. *et al.* (2012) Expansion–contraction of photo-responsive artificial muscle regulated by host–guest interactions. *Nat. Commun.* 3, 1–8
129. Cezar, C.A. *et al.* (2016) Biologic-free mechanically induced muscle regeneration. *Proc. Natl. Acad. Sci. U. S. A.* 113, 1534–1539
130. Pan, Y. *et al.* (2016) Differential growth triggers mechanical feedback that elevates Hippo signaling. *Proc. Natl. Acad. Sci. U. S. A.* 113, E6974–E6983
131. Sunyer, R. and Trepat, X. (2020) Durotaxis. *Curr. Biol.* 30, R383–R387
132. Sunyer, R. *et al.* (2016) Collective cell durotaxis emerges from long-range intercellular force transmission. *Science (80-.)* 353, 1157–1161
133. Wen, J.H. *et al.* (2015) Haptotaxis is cell type specific and limited by substrate adhesiveness. *Cell. Mol. Bioeng.* 8, 530
134. Luo, X. *et al.* (2020) Lymphocytes perform reverse adhesive haptotaxis mediated by LFA-1 integrins. *J. Cell Sci.* 133, jcs242883
135. Cheng, D. *et al.* (2019) Studies of 3D directed cell migration enabled by direct laser writing of curved wave topography. *Biofabrication* 11, 021001
136. Liao, Z. *et al.* (2021) Optogenetics-based localization of talin to the plasma membrane promotes activation of β3 integrins. *J. Biol. Chem.* 296, 100675
137. Tang, W.-C. *et al.* (2022) Optogenetic manipulation of cell migration with high spatiotemporal resolution using lattice lightsheet microscopy. *bioRxiv* Published online January 2, 2022. https://doi.org/10.1101/2022.01.02.474058
138. Messal, H.A. *et al.* (2019) Tissue curvature and apicobasal mechanical tension imbalance instruct cancer morphogenesis. *Nature* 566, 126–130
139. Kim, S. *et al.* (2021) Harnessing mechanobiology for tissue engineering. *Dev. Cell* 56, 180–191
140. Bauer, A. *et al.* (2021) pyTFM: A tool for traction force and monolayer stress microscopy. *PLoS Comput. Biol.* 17, e1008364
141. Gómez-González, M. *et al.* (2020) Measuring mechanical stress in living tissues. *Nat. Rev. Phys.* 2, 300–317
142. Hill, R. (1950) C. A theory of the plastic bulging of a metal diaphragm by lateral pressure. *Lond. Edinb. Dublin Philos. Mag. J. Sci.* 41, 1133–1142
143. Tambe, D.T. *et al.* (2011) (2011) Collective cell guidance by cooperative intercellular forces. *Nat. Mater.* 106, 469–475
144. Elosegui-Artola, A. *et al.* (2022) Matrix viscoelasticity controls spatio-temporal tissue organization. *bioRxiv* Published online January 20, 2022. https://doi.org/10.1101/2022.01.19.476771
145. Mason, B.N. and Reinhart-King, C.A. (2013) Controlling the mechanical properties of three-dimensional matrices via non-enzymatic collagen glycation. *Organogenesis* 9, 70–75
146. Sarrigiannidis, S.O. *et al.* (2021) A tough act to follow: collagen hydrogel modifications to improve mechanical and growth factor loading capabilities. *Mater. Today Biol.* 10, 100098
147. Bhagat, V. and Becker, M.L. (2017) Degradable adhesives for surgery and tissue engineering. *Biomacromolecules* 18, 3009–3039
148. Isomursu *et al.* (2022) Directed cell migration towards softer environments. *Nat. Mater.* Published online July 11, 2022. https://dx.doi.org/10.1038/s41563-022-01294-2